

### 15.3 Printed Electronic Nose Vapor Sensors for Consumer Product Monitoring

Vivek Subramanian, Josephine B. Lee, Vincent H. Liu, Steven Molesa

University of California, Berkeley, CA

Printed organic semiconductors have received attention for low-cost applications such as displays and RFID tags. Unfortunately, current performance falls short of the needs of these applications, and therefore, viability is some years off.

An application that ideally matches well to the capabilities of organic electronics is sensors. Organics offer synthetic richness; through chemistry it is possible to produce organic TFTs with tuned sensitivity. By arraying multiple sensor elements, it is possible to obtain signatures that provide high specificity at low cost [1]. This is attractive since it may make in-package food and pharmaceutical monitoring economically feasible. Use of inkjet printing ensures low cost since inkjet offers the capability of easily depositing multiple materials in different locations.

Most organic semiconductors are sensitive to their environment. Unfortunately, they typically show sensitivity to multiple vapors and are therefore nonspecific. Fortunately, specificity may be obtained by arraying TFTs with different channel materials and subsequently pattern matching. At least in the near term, such sensors will likely be used with a silicon-based processing platform. In comparison to an all-silicon nose, such a system offers similar sensitivity (ppm level detection) and specificity (single functional group differentiation) at lower cost. Silicon noses typically require one additional mask per sensor element, and often need many elements for high specificity. The use of printed sensors with high functional specificity eliminates these needs, and should enable the realization of integrated noses with a cost of less than 5 cents ( $>1000\times$  cheaper than existing noses). In the longer term, it should be possible to integrate signal processing within the organic platform itself; indeed, we have already developed robust device models and several workers in the field have demonstrated circuits of suitable complexity to suggest that integrated all-organic sensors are within reach.

A micrograph, device cross-section, and output characteristics are shown in Fig. 15.3.1. All layers in the device are printable, including the polymer dielectric, nanoparticle metal contacts, and organic semiconductor. Channel lengths of  $\sim 20\mu\text{m}$  are achievable. Mobilities of  $\sim 0.2\text{cm}^2/\text{Vs}$  have been demonstrated [2]. More recently,  $\text{VDD} < 10\text{V}$  has been demonstrated, making CMOS compatibility more achievable [3]. The performance of these TFTs is similar to back-gated TFTs fabricated on thermally oxidized silicon. Therefore, these are good vehicles for evaluating performance, and are also used throughout this work. By forming arrays of TFTs with different printed channels, arrayed sensors may be realized.

The use of a bottom-gated architecture ensures that the semiconductor sees maximum exposure to the analyte, increasing sensitivity. Sensitivity of  $\sim 10\text{ppm}$  has been achieved, as shown in Fig. 15.3.2, which shows the fractional change in drive current as a function of analyte exposure [4]. False positives are limited by use of arrays, since the differential signal may be tuned for specificity by choice of appropriate semiconductors. For example, by using two different polythiophenes with different functional groups, divergent responses to the same gas can be produced, as shown in Fig. 15.3.3, which allows production of a strong differential signal.

Upon exposure, a large change in drive current results. This change in drive current may be caused by a combination of changes in both the threshold voltage and mobility, as shown in Fig. 15.3.4. While mobility appears to depend solely on gas exposure,  $V_T$  also shows a time dependency. This is due to a reversible bias-stress effect on TFT threshold voltage [5]. This is a known problem with organic TFTs, and requires circuit-based correction.

To separate the sensor shift due to analyte exposure from the sensor shift due to bias stressing, differential architectures are used, with two identical transistors wired into a bridge. One transistor is protected with an overlying polymer layer. Both transistors are biased at identical voltages, ensuring that the bridge accounts for the bias stress. Upon analyte exposure, only the unprotected transistor shows an additional shift, which may be measured as shown in Fig. 15.3.5. Matching between devices fabricated on a single substrate is very good ( $\sim 5\%$  error) and is preserved for weeks of continuous testing at 100% duty cycle, thus preserving sensor linearity. Temperature sensitivity has also been studied. Sensors do not show irreversible degradation up to  $>120^\circ\text{C}$ . Since both transistors within the bridge are subjected to the same temperature, temperature induced drift in device current is compensated. The signal output from the bridge is fed into a high-impedance amplifier circuit. The output is then converted using a commercial ADC for processing / identification. Given this system topology, it should be possible to implement the entire system on a single chip; indeed, the sensor elements may be printed directly on the chip package.

As a demonstration, the spoilage of wine is studied. Wine spoilage is a known problem in the wine industry, with a non-negligible volume of wine-bottles being subject to return due to on-shelf and in-transit spoilage. Calibration experiments performed with pure ethanol and acetic acid show that differential signals are expected as wine spoils due to the accumulation of acetic acid. Deployment in a wine testing environment verifies this, as shown in Fig. 15.3.6. The extrema on the vertical axis represent the expected response for pure ethanol ( $-2$ ) and pure acetic acid ( $+2$ ). When fresh wine is slowly converted to stale wine, all the device parameters, including mobility, threshold voltage, and drive current, drift upward. All testing has been performed in humid air to loosely match the conditions prevalent during bottling. Wine spoilage detection should therefore be possible in a compact in-situ sensor system, thus attesting to the potential of these sensors for consumer product monitoring.

#### Acknowledgements:

The authors acknowledge M. Heeney, S. Tierney, and I. McCulloch from Merck Chemicals, and J. Liu, A. Murphy, and J. M. J. Fréchet from the UC Berkeley Chemistry Department for provision of some of the materials used.

#### References:

- [1] B. Crone et al, "Electronic Sensing of Vapors Using Organic Transistors," *Appl. Phys. Lett.*, 78, pp. 2229-2231, 2001.
- [2] S. Molesa et al, "A High-Performance All-Inkjetted Organic Transistor Technology," *IEDM Tech. Dig.*, pp. 1072-1073, 2004.
- [3] S. Molesa et al, "Low Voltage Inkjetted Organic Transistors for Printed RFID and Display Applications," *IEDM*, pp. 5.4.1-5.4.4, 2005.
- [4] J. B. Lee et al, "Polythiophene Thin-film Transistor Array for Gas Sensing," *Dev. Res. Conf. Conf. Dig.*, pp. 147-148, 2005.
- [5] J. B. Lee et al, "Stability in OTFT Gas Sensors," *Mat. Res. Soc. Spr. Meeting*, 2005.

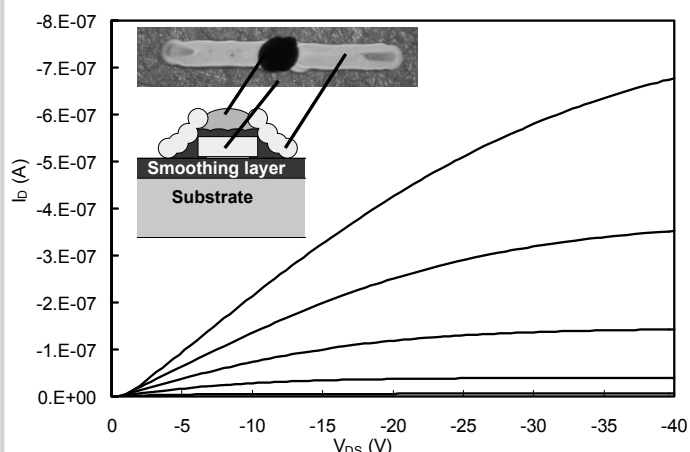


Figure 15.3.1: Micrograph, schematic cross-section, and electrical characteristics of printed TFT (W/L=120 $\mu$ m/45 $\mu$ m).

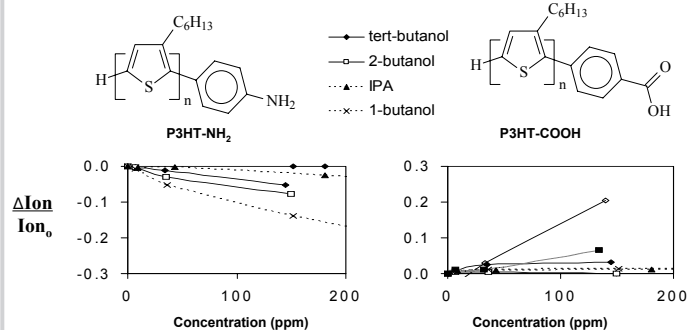


Figure 15.3.3: Response of two different thiophenes (with NH<sub>2</sub> and COOH termination, respectively) to different alcohol vapors, showing opposite trends. This is the basis for array-based specificity enhancement.

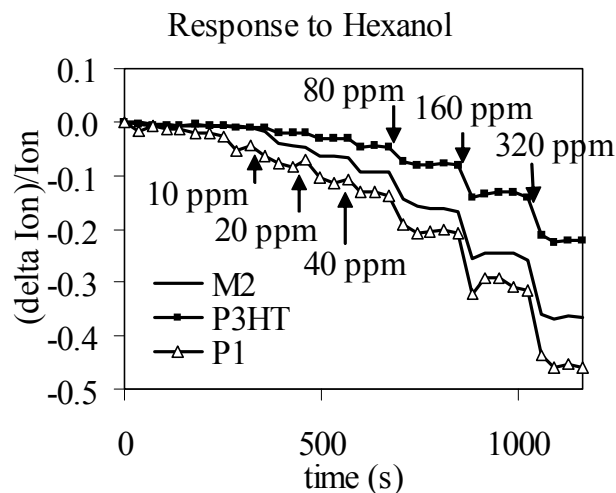


Figure 15.3.2: Response of a 3-element sensor (with an oligothiophene, M2, a polythiophene, P3HT, and a pentacene P1) to hexanol vapors, showing ppm level sensitivity.

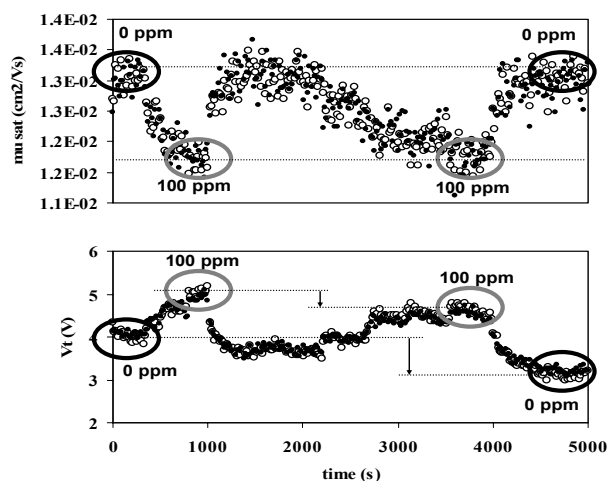


Figure 15.3.4: Sensors show response in both threshold voltage and mobility. While mobility response is highly repeatable over weeks of operation, the VT response is convoluted with bias-stress effects.

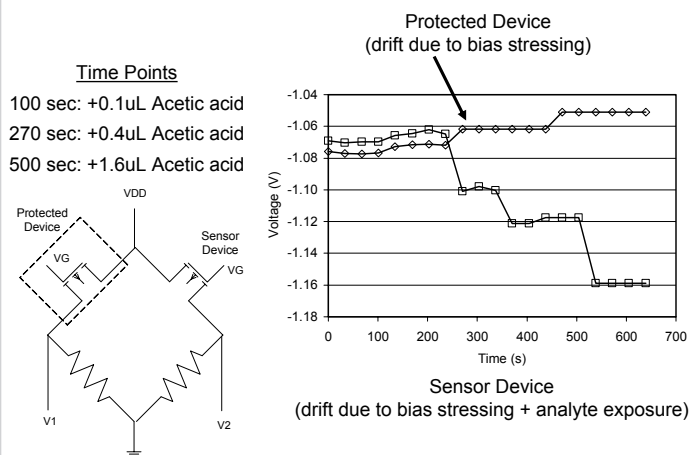


Figure 15.3.5: Use of a bridge architecture to isolate sensor response from bias stress effect.

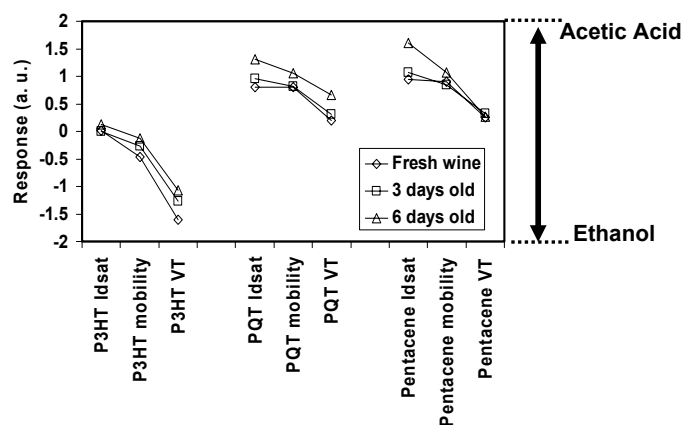


Figure 15.3.6: Sensing of wine spoilage using a 3-element array. The transistor channels are polythiophene (P3HT), polyquaterthiophene (PQT), and pentacene respectively.